


 Cite this: *Chem. Commun.*, 2025, 61, 18108

 Received 13th June 2025,  
 Accepted 25th September 2025

DOI: 10.1039/d5cc03325j

[rsc.li/chemcomm](https://rsc.li/chemcomm)

# Click chemistry enables rapid development of potent sEH PROTACs using a direct-to-biology approach

 Julia Schönfeld,<sup>a</sup> Nick Liebisch,<sup>a</sup> Steffen Brunst,<sup>ab</sup> Lilia Weizel,<sup>a</sup> Stefan Knapp,<sup>id</sup> <sup>acd</sup>  
 Aimo Kannt,<sup>id</sup> <sup>bd</sup> Ewgenij Proschak<sup>ab</sup> and Kerstin Hiesinger<sup>id</sup> \*<sup>a</sup>

The direct-to-biology (D2B) approach enables biological screening of crude reaction mixtures, eliminating the need for purification steps and thereby accelerating drug discovery. In this study, we developed a miniaturized D2B platform for the rapid synthesis of proteolysis targeting chimera (PROTAC) degraders of soluble epoxide hydrolase (sEH). We used copper-catalyzed azide–alkyne cycloaddition and optimized the conditions for 384-well PCR plate applications with 10  $\mu$ L reaction volumes on a 300 nmol scale. This approach enabled the D2B synthesis of 92 crude PROTACs from azide-functionalized CRBN-ligands and alkyne-linked sEH inhibitors. Biological screening using a HiBiT lytic degradation assay identified two hits that were resynthesized and exhibited subnanomolar DC<sub>50</sub> values and degradation efficacy (D<sub>max</sub>). Thus, we established a scalable, cost-effective and time-saving D2B platform for the discovery of PROTACs in very small quantities. This methodology is particularly suitable for early-stage screening and hit validation assessing the degradability of a target.

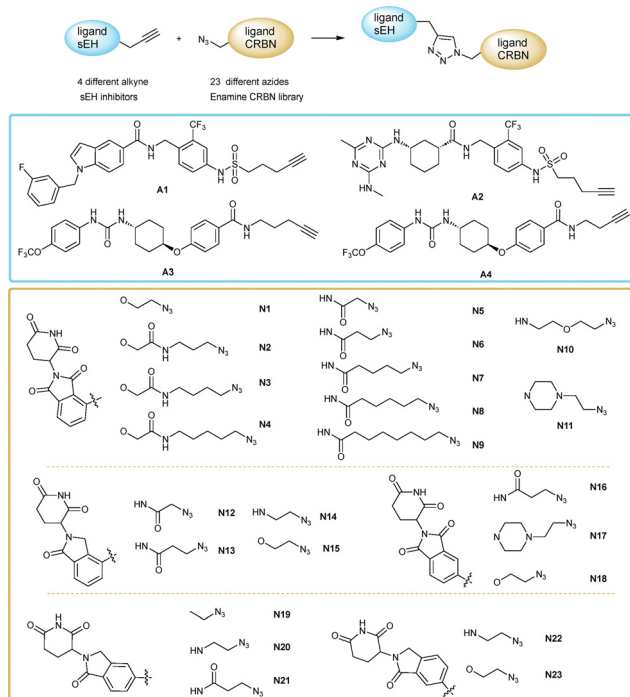
Acceleration of the drug discovery process while ensuring reliability remains a central challenge in medicinal chemistry. One increasingly adopted solution, particularly within the pharmaceutical industry,<sup>1–3</sup> is the direct-to-biology (D2B) approach. This strategy involves evaluating crude reaction mixtures directly in biological assays, eliminating the need for purification steps. This technique dramatically reduces time and resource consumption by enabling fast hit identification, bypassing labour-intensive purification steps, and streamlining the screening workflow. The D2B approach is particularly well suited for the synthesis of proteolysis targeting chimeras (PROTACs). PROTACs are heterobifunctional modalities

that bind to a protein of interest and a E3 ligase to induce degradation of the protein of interest. In PROTAC discovery, hit identification requires a high synthetic effort with limited opportunities for rational design due to the complex nature of PROTAC development.<sup>4</sup> Fast biological testing of the synthesized PROTACs is enabled by the HiBiT technology which allows for high throughput screening for degradation,<sup>5</sup> avoiding time consuming techniques such as Western blotting or ELISA. The efficiency of D2B workflows is further enhanced by miniaturization of chemical reactions, which brings significant benefits such as reduced chemical waste, lower consumption of valuable starting materials and the ability to run high-throughput reactions in parallel in a plate-based format. These improvements accelerate the early stage of hit discovery while maintaining sustainability and cost efficiency. To date, most D2B platforms are based on amide coupling, as this reaction is reliable and typically results in high yields.<sup>1–3</sup> Another simple and robust reaction is the copper-catalysed azide–alkyne cycloaddition (CuAAC, click chemistry), which is ideal for D2B applications as it has a high atom economy, tolerates a broad range of functional groups and requires no extremely hazardous reagents and no heating.<sup>6</sup> In 2017, Wurz and coworkers demonstrated a click chemistry platform for the synthesis of PROTACs (0.1 mmol scale), in which the PROTACs were evaluated for degradation after purification.<sup>7</sup> Che and colleagues have recently shown that click chemistry is suitable for automated synthesis in 1 mL reaction volume within a D2B approach.<sup>8</sup> The present study aims at scaling down this procedure even further and optimizing the click reaction for 10  $\mu$ L reaction volume and a nanomole scale. To evaluate the utility of our platform, we selected soluble epoxide hydrolase (sEH) as a model target due to its therapeutic relevance in the context of inflammation-related diseases<sup>9</sup> and the availability of an in-house degradation assay utilizing HiBiT technology.<sup>5</sup> sEH comprises a C-terminal epoxide hydrolase domain and a structurally distinct N-terminal lipid phosphatase domain, both of which can be concurrently eliminated *via* PROTAC-mediated targeted protein degradation.<sup>10</sup> Notably, Peyman *et al.* demonstrated that an sEH-targeting PROTAC effectively reduces endoplasmic

<sup>a</sup> Institute of Pharmaceutical Chemistry, Goethe University, 60438 Frankfurt am Main, Germany. E-mail: [Hiesinger@pharmchem.uni-frankfurt.de](mailto:Hiesinger@pharmchem.uni-frankfurt.de)
<sup>b</sup> Fraunhofer Institute for Translational Medicine and Pharmacology ITMP, 60596 Frankfurt am Main, Germany

<sup>c</sup> Structural Genomics Consortium (SGC), Buchmann Institute for Life Sciences, 60438 Frankfurt/Main, Germany

<sup>d</sup> Institute for Clinical Pharmacology, Goethe University, 60596 Frankfurt am Main, Germany

**Scheme 1** Detailed presentation of the structures of the library. Top: chemical structures of alkyne-functionalized sEH ligands **A1–A4**. Bottom: chemical structures of azide-functionalized CRBN ligands **N1–N23**.

reticulum (ER) stress and inflammatory markers in hepatic cells and murine liver tissue.<sup>11</sup>

In a previous study, we developed sEH PROTACs using conventional combinatorial chemistry and showed that CRBN-based PROTACs effectively target sEH.<sup>10</sup> This time, however, we aim to take a direct-to-biology approach using a more diverse set of alkynes and azides, in contrast to our previous

study where each PROTAC was first purified before testing. Building on this, we focused on CRBN-targeting ligands and acquired a library of 23 azides (3  $\mu\text{mol}$  each) from Enamine (Scheme 1). Guided by reported sEH PROTACs and sEH inhibitor crystal structures, we designed four sEH inhibitors with terminal alkynes oriented toward the solvent to enable click coupling with the azide library. We targeted the C-terminal epoxide hydrolase domain (sEH-H), known for its well-characterized and accessible binding site. We chose the sEH-H inhibitors t-TUCB and FL217, as these ligands were already successfully used for PROTAC design<sup>10,12</sup> as well as GSK2256294, which is a highly potent sEH-H ligand with excellent pharmacokinetic properties.<sup>13</sup> For the exit of the short branch of the binding pocket, the FL217-based ligand **A1** and the GSK2256294-based ligand **A2** were selected, while the t-TUCB-based ligands **A3** and **A4** were designed to address the exit of the long branch (Scheme 1). For the optimization studies, we chose the reaction of sEH ligand **A1** with Pomalidomide-PEG5-azide (**N24**) or Thalidomide-O-amido-PEG4 (**N25**) to PROTAC **P1** or **P2**, respectively, which has been successful in our previous study.<sup>10</sup>

Using CuI in dichloromethane gave poor conversion (Table 1, entry 1). Switching to  $\text{CuSO}_4 \cdot 5 \text{H}_2\text{O}$  with sodium ascorbate improved the results (entries 2 and 3), and further optimization with a DMF/water mix gave high conversion rates and good yields (entry 5). To avoid the hazardous solvent DMF, we opted for DMSO, a safer, biocompatible solvent whose high boiling point minimizes concentration fluctuations in plate-based reactions. Using the optimized conditions, we downscaled the reaction to 50  $\mu\text{L}$  in a 96-well plate with 60 mM ligand **A1**, resulting in moderate conversion rates (Table 1, entry 7). Switching to a 384-well plate at the same volume restored high conversion, likely due to better solvent surface area (entry 8). Further testing confirmed that the CuAAC reaction is highly concentration-dependent, as reported by Hashimoto *et al.*<sup>14</sup> Lower reactant concentrations decreased the conversion rates (Fig. S1A), so we used 60 or 30 mM

**Table 1** Optimization study of the CuAAC in small volumes

No	N	Eq. Azide	Cu(i) source	Additive	$\mu\text{L}$	Solvent	Time	Conv.	Yield
1	2	1.05	0.2 eq CuI	0.4 eq DIPEA, 0.4 eq HOAc	1000	$\text{CH}_2\text{Cl}_2$	2 h	58:42	20%
2	2	1.05	0.1 eq $\text{CuSO}_4 \cdot 5\text{H}_2\text{O}$	0.1 eq ascorbate, 0.1 eq $\text{PhCO}_2\text{H}$	1000	$t\text{BuOH} : \text{H}_2\text{O} 1 : 2$	2 h	50:50	25%
3	2	1.20	0.1 eq $\text{CuSO}_4 \cdot 5\text{H}_2\text{O}$	0.4 eq ascorbate	1600	$t\text{BuOH} : \text{H}_2\text{O} 1 : 1$	24 h	10:90	45%
4	2	1.10	0.3 eq $\text{CuSO}_4 \cdot 5\text{H}_2\text{O}$	0.3 eq ascorbate	1300	$\text{DMF} : \text{H}_2\text{O} 4 : 1$	16 h	2:98	45%
5	4	1.10	0.3 eq $\text{CuSO}_4 \cdot 5\text{H}_2\text{O}$	0.3 eq ascorbate	1300	$\text{DMF} : \text{H}_2\text{O} 4 : 1$	16 h	2:98	42%
6	4	1.00	0.3 eq $\text{CuSO}_4 \cdot 5\text{H}_2\text{O}$	0.3 eq ascorbate	50	$\text{DMF} : \text{H}_2\text{O} 4 : 1$	16 h	2:98	49%
7 <sup>a</sup>	5	1.00	0.3 eq $\text{CuSO}_4 \cdot 5\text{H}_2\text{O}$	0.3 eq ascorbate	50	$\text{DMSO} : \text{H}_2\text{O} 4 : 1$	16 h	17:83	—
8 <sup>b</sup>	5	1.00	0.3 eq $\text{CuSO}_4 \cdot 5\text{H}_2\text{O}$	0.3 eq ascorbate	50	$\text{DMSO} : \text{H}_2\text{O} 4 : 1$	16 h	2:98	—

<sup>a</sup> 96-well plate. <sup>b</sup> 384-well plate.



(relative to starting material) and reduced the reaction volume in 384-well plates for better mixing. V-shaped wells improved the conversion rates compared to flat-bottomed plates (Fig. S1B and C). High conversion (97–98%) was achieved at 5–10  $\mu\text{L}$  volumes with 150–300 nmol alkyne/azide (Fig. S1C). To test the robustness of the system, we ran the reaction at least three times for each volume and found that conversion rates were more variable when using a 5  $\mu\text{L}$  reaction volume (Fig. S2D).

In parallel, we tested the crude reaction mixtures of our model system (PROTAC **P2**) with our optimized conditions (3 h and 18 h incubation, 300 nM PROTAC/crude) in our previously reported HiBiT lytic assay system (Fig. S1E).<sup>10</sup> In this cell-based assay, bioluminescence is used to measure the degradation of sEH. The sEH protein is tagged with a small peptide fragment of NanoLuciferase (NanoLuc) called HiBiT. With addition of the LgBiT peptide, which marks the residual scaffold of NanoLuc, and the substrate, bioluminescence is generated. The more sEH is degraded, the less bioluminescence is detected. We observed reduced degradation of sEH by PROTACs tested with lower conversion rates, most likely because unreacted alkyne competes with the lower concentrations of PROTAC for sEH binding. To assess potential cytotoxicity, we tested the copper sulfate/ascorbate system at assay concentrations and observed only minor luminescence changes (<5%; Fig. S1E) and no effect on cell viability (Fig. S2). With the optimized reaction conditions in hand, we performed the parallel synthesis of 92 PROTACs from the sEH ligands functionalized with an alkyne **A1**–**A4** and the purchased azide library (Scheme 1). We prepared DMSO stock solutions for the azide- and alkyne-functionalized ligands and water stock solutions for  $\text{CuSO}_4 \cdot 5 \text{H}_2\text{O}$  and sodium ascorbate. The respective volumes of azide, alkyne, copper(I) source and reducing agent were added to the 384-well PCR plate and the plate was sealed with aluminum foil. The plate was shaken overnight on a plate shaker, and 1  $\mu\text{L}$  of each reaction mixture was used to determine the conversion (HPLC-MS). Another 1  $\mu\text{L}$  of the crudes was used to prepare the stocks for biological evaluation. In this setup, we observed a mean conversion of 85%, with the lowest conversion being 28%. We tested all crude samples with a 300 nM concentration in the HiBiT lytic assay, as this was an effective PROTAC concentration in our previous study, and were able to detect degradation of sEH screening the crude reaction mixtures (Fig. 1A–D). As a hit threshold, we chose a degradation of at least 50%. To confirm reproducibility, we re-tested the synthesized click library in the HiBiT assay and observed the same degradation pattern and hits.

We then repeated the click reaction using **A1** and **A3** (since **A2** and **A4** yielded no hits), resulting in a slightly lower median conversion of 77% (Fig. S3). This is due to the two azides not being transferred to the reaction plate, leading to only the alkynes being detectable in the HPLC traces. Excluding these, the average conversion was 82%, matching the initial experiment. We were able to confirm the identified hits in the HiBiT lytic assay as before. We obtained two hits with only one sEH scaffold (**A3**). PROTACs **P3** and **P4**, which are combinations of sEH ligand **A3** and **N23**, a lenalidomide-derived CRBN ligand with a short alkyl chain as the linker, and **N17**, a pomalidomide

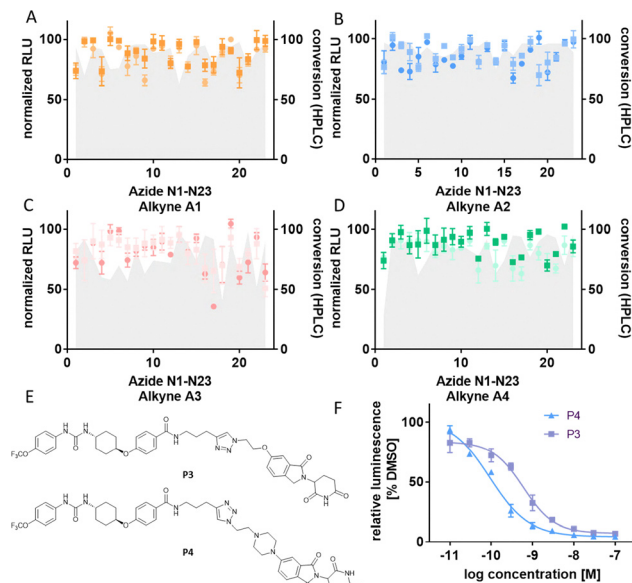


**Fig. 1** (A)–(D) Degradation activities of the crude mixtures in a HiBiT lytic assay. Cells were treated with 300 nM of the crude mixtures for 18 h ( $n = 2$  in triplicates, error bars in standard deviation (SD)); (E) structure of hit PROTACs; (F): concentration-dependent degradation ability of purified hits **P3** and **P4** ( $n = 2$  in triplicates, error bars in SD).

substructure with a piperazine moiety in the linker. To confirm our hits, we resynthesized **P3** and **P4** (Fig. 1E), purified the compounds by preparative HPLC, and evaluated them in the HiBiT lytic assay. We measured the dose–response at different incubation times and determined the  $D_{\text{max}}$  and  $DC_{50}$ . **P3** exhibited a  $pDC_{50}$  of  $9.17 \pm 0.06$  and a  $D_{\text{max}}$  of  $91 \pm 2\%$  and **P4** exhibited a  $pDC_{50}$  of  $10.3 \pm 0.2$  and a  $D_{\text{max}}$  of  $96 \pm 1\%$ , both after 18 h incubation (Fig. 1F). After 6 h of incubation, we as well observed a significant degradation of sEH (Fig. S4). The addition of control compounds, comprising an sEH inhibitor, a proteasome inhibitor, and a CRBN ligand, reversed the degradation effect (Fig. S5). In a spiking experiment, adding sEH ligand **A3** to pure PROTACs **P3** and **P4** reduced degradation as higher amounts of **A3** outcompete the PROTAC from the binding site of sEH-H (Fig. S6), consistent with earlier results (Fig. S1E). This effect may cause false negatives, though potent PROTAC **P4** was discovered as a hit despite moderate conversion. Lastly, we assessed the metabolic stability in rat liver microsomes and observed minimal degradation (<15%) after one hour of incubation (Fig. S7).

In this study, we successfully developed and optimized a highly miniaturized D2B platform for the synthesis and biological evaluation of PROTACs targeting sEH, utilizing click chemistry (CuAAC reaction). Our results demonstrate that the CuAAC reaction can be effectively scaled down to reaction volumes as low as 10  $\mu\text{L}$  while maintaining high conversion rates, provided appropriate plate formats and reagent concentrations are used. By applying this workflow to a thalidomide-based azide library and alkyne-functionalized sEH inhibitors, we achieved the parallel synthesis of 92 unpurified potential PROTACs. Direct screening of crude reaction mixtures in a HiBiT lytic degradation assay



led to two hits that were resynthesized. These PROTACs exhibited low nanomolar to subnanomolar  $DC_{50}$  values and degraded sEH with a  $D_{max}$  of 90–96%, validating the biological relevance of the hits despite moderate reaction conversions in some cases. However, we also observed that the residual unreacted alkyne-functionalized sEH ligand can interfere with degradation activity, underscoring the importance of reaction completeness in D2B workflows to avoid false negatives. Overall, our findings establish a scalable, cost-effective, and time-efficient platform for the discovery of PROTAC degraders in ultra-low volumes. This methodology is particularly suited to evaluate the “PROTACability” of a protein of interest for which ligands are available, as well as for early-stage screening and hit validation. However, in this study we relied on a purchased small CRBN ligand library with only moderate complexity. To increase diversity and complexity in the linker and E3 ligase ligands, a more diverse library will be established and evaluated in our group in the future.

Concept: J. S., E. P., and K. H.; funding acquisition: A. K. and E. P., investigation: J. S., N. L., S. B., J. S., K. H., and L. W.; methodology: J. S., K. H., S. K., and E. P.; project administration: K. H.; writing the original draft: J. S. and K. H.; supervision: K. H.; writing – review and editing: S. K., A. K., and E. P.; manuscript review: all authors.

We are grateful to Astrid Kaiser for conducting the metabolic stability experiments. This research was supported by DFG (Sachbeihilfe 530858826 to E. P.) and by the Proximity-inducing Drugs platform of the Fraunhofer Cluster of Immune Mediated Diseases. N. L., S. K. and K. H. are grateful for support by the translational cancer program of the Deutsche Krebshilfe/German Cancer Aid TACTIC (70115201). A. K. was supported by the Leistungszentrum Innovative Therapeutics (TheraNova) funded by the Fraunhofer Society and the Hessian Ministry of Science and Art.

## Conflicts of interest

There are no conflicts to declare.

## Data availability

The data supporting this article have been included as part of the supplementary information (SI). Supplementary information is available. See DOI: <https://doi.org/10.1039/d5cc03325j>

The preparation of the HiBiT cell lines and the synthesis of alkyne **A1** have been previously reported.<sup>10</sup>

## Notes and references

- 1 R. Stevens, H. E. P. Palmer, A. H. Miah and G. A. Burley, *J. Org. Chem.*, 2025, **90**, 2192–2200.
- 2 R. Stevens, E. Bendito-Moll, D. J. Battersby, A. H. Miah, N. Wellaway, R. P. Law, P. Stacey, D. Klimaszewska, J. M. Macina, G. A. Burley and J. D. Harling, *J. Med. Chem.*, 2023, **66**, 15437–15452.
- 3 M. P. Plesniak, E. K. Taylor, F. Eisele, C. M. B. K. Kourra, I. N. Michaelides, A. Oram, J. Wernevik, Z. S. Valencia, H. Rowbottom, N. Mann, L. Fredlund, V. Pivnytska, A. Novén, M. Pirmoradian, T. Lundbäck, R. I. Storer, M. Pettersson, G. M. de Donatis and M. Rehnström, *ACS Med. Chem. Lett.*, 2023, **14**, 1882–1890.
- 4 D. A. Nalawansha and C. M. Crews, *Cell Chem. Biol.*, 2020, **27**, 998–1014.
- 5 A. S. Dixon, M. K. Schwinn, M. P. Hall, K. Zimmerman, P. Otto, T. H. Lubben, B. L. Butler, B. F. Binkowski, T. Machleidt, T. A. Kirkland, M. G. Wood, C. T. Eggers, L. P. Encell and K. V. Wood, *ACS Chem. Biol.*, 2016, **11**, 400–408.
- 6 V. V. Rostovtsev, L. G. Green, V. V. Fokin and K. B. Sharpless, *Angew. Chem., Int. Ed.*, 2002, **41**, 2596–2599.
- 7 R. P. Wurz, K. Dellamaggiore, H. Dou, N. Javier, M.-C. Lo, J. D. McCarter, D. Mohl, C. Sastri, J. R. Lipford and V. J. Cee, *J. Med. Chem.*, 2018, **61**, 453–461.
- 8 J. Chen, M. Wu, J. Mo, J. Hong, W. Wang, Y. Jin, X. Mao, X. Liao, K. Li, X. Yu, S. Chen, S. Zeng, W. Huang, H. Xu, J. Wu, J. Cao, Y. Zhou, M. Ying, C. Zhu, Q. He, B. Zhang, N. Lin, X. Dong and J. Che, *J. Med. Chem.*, 2025, **68**, 8010–8024.
- 9 (a) A. Gregory, C. Tang and F. Fan, *Neural Regener. Res.*, 2025, **20**, 2585–2586; (b) J. Hu, S. Dziumbala, J. Lin, S.-I. Bibli, S. Zukunft, J. de Mos, K. Awwad, T. Frömel, A. Jungmann, K. Devraj, Z. Cheng, L. Wang, S. Fauser, C. G. Eberhart, A. Sodhi, B. D. Hammock, S. Liebner, O. J. Müller, C. Glaubitz, H.-P. Hammes, R. Popp and I. Fleming, *Nature*, 2017, **552**, 248–252; (c) J. I. Obeme-Nmom and C. C. Udenigwe, *Curr. Opin. Food Sci.*, 2024, **57**, 101174.
- 10 J. Schönfeld, S. Brunst, L. Ciomirtan, L. Willmer, M. A. Chromik, A. Kumar, T. Froemel, N. Liebisch, A. Hackspacher, J. H. M. Ehrler, L. Wintermeier, C. Hesse, J. Fiedler, J. Heering, H. Freitag, P. Zardo, H.-G. Fieguth, A. Brüggerhoff, J. Jakob, B. Häupl, L. Weizel, A. Kaiser, M. Schubert-Zsilavecz, T. Oellerich, I. Fleming, N. H. Schebb, R. Fürst, A. Kannt, S. Knapp, E. Proschak and K. Hiesinger, *J. Med. Chem.*, 2025, **68**, 13728–13749.
- 11 M. Peyman, E. Barroso, A. L. Turcu, F. Estrany, D. Smith, J. Jurado-Aguilar, P. Rada, C. Morisseau, B. D. Hammock, Á. M. Valverde, X. Palomer, C. Galdeano, S. Vázquez and M. Vázquez-Carrera, *Biomed. Pharmacother.*, 2023, **168**, 115667.
- 12 (a) Y. Wang, C. Morisseau, A. Takamura, D. Wan, D. Li, S. Sidoli, J. Yang, D. W. Wolan, B. D. Hammock and S. Kitamura, *ACS Chem. Biol.*, 2023, **18**, 884–896; (b) K. Nakane, C. Morisseau, P. D. Dowker-Key, G. Benitez, J. T. Aguilan, E. Nagai, S. Sidoli, B. D. Hammock, A. Betteaieb, K. Shinoda and S. Kitamura, *ACS Med. Chem. Lett.*, 2024, **15**, 1891–1898.
- 13 (a) P. L. Podolin, B. J. Bolognese, J. F. Foley, E. Long, B. Peck, S. Umbrecht, X. Zhang, P. Zhu, B. Schwartz, W. Xie, C. Quinn, H. Qi, S. Sweitzer, S. Chen, M. Galop, Y. Ding, S. L. Belyanskaya, D. I. Israel, B. A. Morgan, D. J. Behm, J. P. Marino, E. Kurali, M. S. Barnette, R. J. Mayer, C. L. Booth-Gentle and J. F. Callahan, *Prostaglandins Other Lipid Mediators*, 2013, **104–105**, 25–31; (b) F. F. Lillich, S. Willems, X. Ni, W. Kilu, C. Borkowsky, M. Brodsky, J. S. Kramer, S. Brunst, V. Hernandez-Olmos, J. Heering, S. Schierle, R.-I. Kestner, F. M. Mayser, M. Helmstädter, T. Göbel, L. Weizel, D. Namgaladze, A. Kaiser, D. Steinhilber, W. Pfeilschifter, A. S. Kahnt, A. Proschak, A. Chaikuad, S. Knapp, D. Merk and E. Proschak, *J. Med. Chem.*, 2021, **64**, 17259–17276; (c) A. Shrestha, P. T. Krishnamurthy, P. Thomas, B. D. Hammock and S. H. Hwang, *J. Pharm. Pharmacol.*, 2014, **66**, 1251–1258.
- 14 Y. Ogasawara, Y. Murai, Y. Sakihama, Y. Hashidoko and M. Hashimoto, *Int. J. Org. Chem.*, 2012, **02**, 302–304.

